Giemsa-based cytological assessment of area, shape and nucleus:cytoplasm ratio of goblet cells of rabbit bulbar conjunctiva

Doughty, Michael

Published in:
Biotechnic and Histochemistry

DOI:
10.1080/10520295.2016.1247988

Publication date:
2016

Document Version
Author accepted manuscript

Giemsa-based cytological assessment of goblet cell area, shape and nucleo-cytoplasmic ratio – application to rabbit bulbar conjunctiva

MJ Doughty

Department of Vision Sciences, Glasgow-Caledonian University, Cowcaddens Road, Glasgow G4 OBA

Running head (short title) **Giemsa-based cytology for goblet cell morphometry**

Correspondence to: MJ Doughty, Department of Vision Sciences, Glasgow-Caledonian University, Cowcaddens Road, Glasgow G4 OBA. E-mail: m.doughty@gcal.ac.uk

Abstract
Goblet cells were visualized in specially-prepared impression cytology specimens (from bulbar conjunctiva of the rabbit eye) using Giemsa staining. Highly magnified images were used to generate outlines of the cells and their characteristic eccentrically-located nuclei. From sets of 10 cells from 15 different cytology specimens, goblet cells were found to have longest dimensions averaging 16.7 +/- 2.3 microns (+/- SD), shortest dimensions of 14.4 +/- 1.8 microns and nucleus dimensions of 6.3 +/- 0.8 microns. All these dimensions were smaller than those in surrounding epithelial (non-goblet) cells. The goblet cells were ellipsoidal in shape with the longest:shortest ratio averaging 1.169. The measured goblet cell areas ranged from 108 to 338 sq. microns (average 193 +/- 50 sq. microns) and could be reliably predicted from the longest and shortest dimensions (r squared = 0.903). Goblet cell nuclei had areas from 15 to 58 sq. micron (average 33 +/- sq. microns) with the nucleo-cytoplasmic area fraction being very predictably greater in smaller goblet cells and smaller in the larger goblet cells (correlation = -0.817). The nuclei were estimated to occupy an average of 9.5 % of the cell volume. The differences in size, shape and nucleo-cytoplasmic (N/C) ratio may reflect changes in goblet cell maturation.

Key words: conjunctiva, epithelial cells, Giemsa, goblet cells, morphometry, rabbit

[Introduction]
Mucous epithelia are found at certain locations throughout the body characterized by their being a layer of cells surrounding a liquid-filled cavity (e.g. gut) or adjacent to a liquid layer (e.g. respiratory and nasal epithelia, as well as the conjunctival epithelium). At the interface between the epithelial cells and the liquid layer is some type of mucus layer, the bulk of which is produced by a specialized cell type found within the epithelia, namely the goblet cell. These cells, given the eponym because of their unusual goblet or cup-like shape that can be seen in histology sections of these epithelia, are uniquely specialized in that they synthesise and then secrete mucins (Forstner 1995; Birchenough et al. 2015). It appears to be an accepted fact that these cells arise from precursor stem cells, progressively mature and ascend (or extend) to the apical surface of the mucous epithelia so as to be able to discharge their mucus content into the fluid layer (Forstner 1995; Rose and Voynow 2006; Johansson 2012; Birchenough et al. 2015). There is a similar presumption that there is a step-wise process of maturation of goblet cells (Forstner 1995; Karam 1999; Kim & Ho 2010) and that there are a certain number of goblet cells within a defined region or area of mucous epithelia, but that there can be too many (i.e. hyperplasia) (Boucherat et al. 2013) or too few (hypoplasia or deficiency of) goblet cells. It has also been noted that individual goblet cells can have different sizes (areas) (Kandori et al. 1996; Kim and Ho 2010) (i.e. be smaller or larger), that goblet cells can be enlarged (Carrillo et al 2015) or be ‘dilated’ (Stringer et al. 2009), but without clear indications being provided as to why such differences (metaplasia) might be apparent.

From this general perspective, there could be some predictable dynamics to the presence and appearance of goblet cells in mucous epithelia. For example, as the cells migrate through their respective epithelia, are there predictable size and / or shape changes and are these any different in epithelia seen to have normal numbers of goblet cells or abnormally low or high density of these cells ?. Similarly, as these cells develop from precursor cells, are there predictable changes in the size of the goblet cells during maturation ?.

To address such issues, measurements need to undertaken on goblet cells, as opposed to simply estimating their numbers (density) or actually counting them. This represents a substantial departure from the vast majority of studies on goblet cells which are usually simply viewed at low magnification in histological sections after staining with mucus-visualizing

stains such as periodate-Schiff (PAS) or Alcian Blue. Notwithstanding, a few measurements (from histological sections) have been reported for the goblet cell diameter (Martins et al. 2015), the cross-sectional area, length and width of goblet cells (Kumari et al. 2009) or estimates of goblet cell volume (Mercer et al. 1994). Similar estimates of cross sectional area of individual goblet cells have been based on measurements of the length (major axis) and width (minor axis) with the two measures then averaged and used to calculate an area (Kandori et al. 1996), and such dimensional measurements have also been used as the basis to assess goblet cell shape 'eccentricity' in relation to overall size of the cells, i.e. how spherical or elongated the cell profiles might appear to be (Halm and Halm 2000).

None of these studies and reports, however, provide much detail on the range of goblet cell sizes seen neither do they address the possible dynamic changes in the goblet cells where, for example, the relative area occupied by the mucin (mucus) would be expected to change in relation to the extent of maturation. The reason for this is not only that the cells are usually viewed at a magnification that is not sufficient for reliable measurements of individual cells to be made but also that the use of mucin-visualizing stains obscures intra-cellular detail. An alternative approach is to use cytology specimens stained with Giesma that reveals the goblet cell outline and a fairly densely staining eccentrically-located nucleus (Spurzem et al. 1991; Lin et al. 1998; Pagliuca et al. 2016). The goblet cells show this outline and appear as balloon-like features distinctly different from other epithelial cells when the samples are taken using a special technique called impression cytology (Roth et al. 1988; Rath et al. 2006; Doughty 2011, 2012a,b, 2015a,b; Colorado et al. 2016).

In the present study, the approach used to assess the goblet cells was with the use of Giemsa on impression cytology samples such that the cell size could be measured (from its outline) and also the nucleus size such that, for the first time, the nucleo-cytoplasmic features of these cells could be assessed in detail.

Materials and Methods

Animal source, care and collection of eye tissue

The animal use and all protocols were in accord with the Association for Research in Vision and Ophthalmology (ARVO) resolution on the Use of Animals in Research, and were approved by a local animal care committee at the University of Waterloo, Canada (Doughty 2014, 2015a). 15 female Dutch Belt pigmented rabbits, aged between 9 to 11 weeks (1.9 to 2.4 kg body weight) were initially quarantined for 7 to 10 days to check that there were no obvious clinical signs of ocular, nasal or GI tract disease. Individual animals were then euthanized with *i.v.* pentobarbital sodium, generally being designated for use in separate ex vivo experiments.

Impression cytology

Immediately after euthanasia, the upper eyelid of the left eye of the rabbits was carefully pushed open and lifted and then a 10 mm diameter sterile filter mounted on a plastic support ring (Millicell®-CM filter unit 0.4 PICM 012550 with the Biopore® membrane, Millipore, Co. Cork, Ireland) was firmly applied onto the exposed superior-temporal bulbar conjunctiva (over the white of the eye) with the filter clear of the edge of the cornea. After a couple of seconds, the filter was removed, allowed to air dry for 2 to 5 minutes and then a single drop of fixative solution applied, and left for 15 min at room temperature. This fixative was a 2 % solution of glutaraldehyde, freshly prepared in 80 mM sodium cacodylate buffer, pH 7.2 to 7.4, 320 to 340 mOsm/L. The filter units were later stained by immersion in 99 % methanol for 2 min, then in distilled water for 1 min and finally in Giemsa solution (product number G032, Sigma, Kingston-upon-Thames, UK) for 2 min. Following previous protocols, the surface of the filters was examined by light microscopy and selected regions photographed using a 20 X microscope stage

objective lens (medium power field, 200 X final magnification, field size 0.14 mm^2) (Doughty 2012a, 2015a).

Cell morphometry

The images were projected onto a wall screen at a final magnification of around 1000 X (Figure 1) so that an overlay (with a 100 μm scale bar) could be generated to facilitate measurements of cell and nucleus dimensions and their areas. These were measured by planimetry using a commercial digitizer pad (DigiPro™, Elstree Computing, London) with dimensional measurements being routinely made to a resolution of 0.5 μm, and area measures to 2 μm^2.

Statistical analysis

All data were entered into spreadsheets in Systat™ (Systat, IL) for calculation of global statistics (mean, SD) with normality of data sets being checked using the Shapiro-Wilk default (as included in Systat) with a value of > 0.05 being considered normal. For comparisons between data sets two-sample t-tests or a non-parametric rank order Friedman test was used, with a statistical difference being considered if $p = 0.05$ or less. Inter-dependence of some of the morphological variables was undertaken using simple correlations, including generating a Spearman correlation coefficient (r_s).

Results

Overall features of the impression cytology images

For the 15 conjunctival impression cytology (CIC) specimens obtained from different rabbits, but at the same anatomical location on the conjunctiva, there were locations across the filter surfaces where there was a mixture of epithelial (non-goblet) cells and goblet cells (Figure 1 and Figure 2B). The projected image serves to highlight the selected regions on the filter surface that were relatively lightly stained such that individual epithelial cells were readily discerned based on their nucleus and cytoplasm staining, and numerous goblet cells were also evident (see below). The image projection shown in Figure 1 is presented to emphasise the extent of cell image magnification used (evident from the hand shown) and the actual process of drawing selected ell outlines onto an overlay. Other regions of the filter surface that were much more densely stained, even to the extent that individual epithelial cells could not be discerned because of substantial overlapping of the stained regions, were avoided even though the goblet cells were still very apparent. For all filters, two representative regions suitable for morphometry were selected.

All filters included regions where just a single layer of largely non-overlapping epithelial (non-goblet) cells were present (see Figure 2A) as well as regions where the epithelial cells were more compact and usually slightly overlapping but where various numbers of goblet cells were present (see Figure 2B). The projected image (Figure 1) shows features similar to Figure 2B in which it can be seen that the Giemsa stain reveals the nuclei of many hundreds of cells across the field of view. Most of these cells, with obviously stained and more centrally located nuclei, were in close contact with each other and appeared flat. However, in marked contrast, a certain proportion of the cells did not appear flat (but rather balloon-like) and quite often could be seen to have a smaller and eccentrically-located nucleus; these are the goblet cells (see Figure 1 and further enlarged region shown in 2A). Subjectively, the 3-D nature of the goblet cells visualized with Giemsa may be more apparent in black-and-white image (Figure 2B) but the original color image was used for projection. These same cells also stain substantially with periodate-Schiff (not shown). The goblet cells chosen for outlining had to have a distinct cell outline and the nucleus outline also needed to be clearly evident.

Morphological features and size of epithelial (non-goblet) cells versus goblet cells

For all specimens, two representative photographs were taken to allow for objective assessments of the goblet cells and non-goblet cells. Representative regions of these are shown in Figure 2. In Figure 2A is shown some non-goblet epithelial cells most of which have similar overall sizes and a prominent centrally-located nucleus. These cells appeared flat. These types of regions were where only the most superficial ones of the conjunctival epithelium had adhered to the filter. If this later of attached cells was completely uniform, an intact monolayer of cells would be seen. However, some small gaps (spaces) between cells were routinely evident and these types of images allowed for unambiguous outlining of the epithelial cells from which measurements could be taken to establish whether these non-goblet cells were normal or abnormal (see later). These epithelial cells were not circular in profile but usually slightly elongated so that a longest dimension and shortest dimension could be measured. The nuclei were rounder in profile and only the longest dimension was measured. In Figure 2B is shown a region of a filter surface where more than one layer of cells had adhered to the filter such that there were no gaps, all of the cells appeared much more crowded together and it was not possible to actually define the edges of the epithelial (non-goblet) cells. One explanation for this overall appearance is the result, in part, of more than one layer of cells being collected onto the filter (see discussion). However, such images now show the presence of the balloon- or sphere-like goblet cells where the outline was distinct and a certain proportion of them were seen to have a well-demarcated (and staining) nucleus. As highlighted, these nuclei in the goblet cells were usually distinctly smaller than those in the surrounding epithelial cells. The presence, or apparent absence, of a nucleus in the goblet cells is purely a consequence of the fine focus adjustment so that with a change in this other goblet cells with nuclei would be apparent. This characteristic serves to emphasize the 3-D nature of the goblet cell profile seen in the impression cytology specimens. The goblet cells were usually ovoid in shape so that, as with epithelial cells, a longest and shortest dimension could be measured as well as the apparent area.

From images of the type shown in Figure 2A, 10 of the best resolved epithelial cells were selected and outlined. The same was done for the best-resolved goblet cells in images of the type shown in Figure 2B, so as to generate a balanced set of data for comparisons between epithelial (non-goblet) and goblet cells.

Overall, the epithelial cells had longest dimensions ranging from 13.9 to 31.7 μm and shorter dimensions from 12.7 to 25.1 μm to give group mean values (from the 15 sets of 10 cells) of 19.2 ± 2.9 and 16.7 ± 2.4 um (mean ± SD respectively). For goblet cells, these ranges were from 11.8 to 23.1 μm for the longest dimension and 10.5 to 19.1 μm for the shorter dimension, with group means of 16.7 ± 2.3 and 14.4 ± 1.8 μm respectively (± SD). The data sets were not normally distributed and a Friedman test showed that both the dimensional value sets were statistically different ($p < 0.001$) when comparing epithelial (non-goblet) cells with the goblet cells, i.e. the goblet cells were slightly smaller. While this feature is not apparent in Figure 1, it should be noted that measures of epithelial cells were not undertaken from this type of image as the edges of the epithelial cells could not been seen because of slight cell-cell overlap.

Overall, the goblet cells had a reasonably homogeneous distribution of values for the longest dimension (Figure 3A) and the shortest dimension (not shown) and the mean value for the average ‘diameter’ [i.e. (long + short)/2)] was 15.5 ± 1.9 um. The shape of most of the goblet cells was distinct in that they were not round but ‘ovoid’ with an average shape factor (long:short, L:S ratio) of 1.169 ± 0.091 (range 1.000 to 1.417) (Figure 3B).

For epithelial cells, the longest dimension of the nuclei averaged 8.1 ± 1.0 μm (range 5.3 to 10.8 um), while for goblet cells this value was smaller at 6.3 ± 0.8 μm (range 4.6 to 8.3

μm). As with cell dimensional measures, the nucleus size (based on length) was distinctly smaller in the goblet cells ($p < 0.001$).

Measured area and estimated goblet cell area and volume

A range of apparent areas of the goblet cells was seen. As shown in Figure 4A, the distribution of the measured area values was broadly unimodal, although was not normally distributed ($p = 0.002$). The overall area value was 200 ± 55 μm^2 (mean ± SD, range 86 to 362 μm^2). The cell areas of the epithelial (non-goblet) cells averaged 269 ± 78 μm^2 (range from 127 to 608 μm^2), a set of values that was statistically larger than those of the goblet cells ($p < 0.001$).

Alternatively, the areas of the goblet cells could be reliably estimated by using the averaged dimensional values, the mean cell 'diameter' (Figure 4B). The correlation between the measured area values and the estimated one was very high ($r^2 = 0.903$, $r_s = 0.920$), with the estimated area being 193 ± 50 μm^2 (range 108 to 338 μm^2). Similarly, the longest dimension of the goblet cells also was a good predictor of the area value (Figure 4C, $r_s = 0.960$).

Using the dimensional values, estimates can also be made of the volume of the spheroid-shaped goblet cells, yielding values between 813 and 4098 μm^3, mean 1885 ± 728 μm^3.

Nucleus characteristics and nucleo-cytoplasmic fraction estimates

For the goblet cells the measured nucleus area values were between 13 to 58 μm^2 (mean 33 ± 8 μm^2), a set of values that were distinctly smaller than those measured for the epithelial (non-goblet) cells (mean 54 ± 12 μm^2 , range 19 to 83 μm^2); these nucleus area values were statistically smaller in the goblet cells ($p < 0.001$).

The distribution of the measured area values for the goblet cell nuclei was not homogeneous (Figure 5A) and suggestive of two sub-populations of nuclei (based on size) with some being smaller and others larger. Notwithstanding, there was a very predictable inter-relationship between the measured goblet cell area and the relative area occupied by the nucleus (Figure 5B) with this proportional area being greater in the smaller goblet cells. Overall, the nuclei could occupy almost half the cell area (seen in profile, with a nucleo-cytoplasmic area fraction as high as 0.484) or only a very small area (with the nucleo-cytoplasmic area fraction being as low as 0.047). The overall inter-dependency of the nucleo-cytoplasmic fraction (ratio) to cell size (area) was highly statistically significant ($r_s = - 0.817$, $p < 0.001$) with a logarithmic function appearing to provide the best fit, at least subjectively. The effect observed cannot be simply accounted for in terms of a cell size-related difference in nucleus size ($p > 0.05$, $r^s = - 0.208$).

The measured values for nucleus size (dimension) can also be used to both estimate the nucleus volume and a nucleo-cytoplasmic volume fraction. The nucleus volume estimates ranged from 52 to 309 μm^3 (mean 141 ± 53 μm^3) yielding nucleo-cytoplsmic volume estimates of between 0.016 to 0.265 (mean 0.095 ± 0.050).

Discussion

These studies are presented to support a perspective that goblet cells can have some predictable dynamic differences. As indicated in the introduction, little actual information (data) appears to be available on the size and shape of goblet cells, and there has been little obvious discussion on any nucleus (or cell) dynamics that could underpin any morphological differences in these cells (Rose and Voynow 2006; Johansson 2012; Birchenough et al. 2005; Karan 1999; Kim and Ho 2010]. In line with higher magnification light microscope based histology with nuclear staining which can show the presence of a basally-located nucleus in mucous cells (Kumari et al. 2009; Schroeder et al., 2012), typical schematic presentations of the goblet cells (and their

precursors for some mucous epithelia) show a cell with a small basally-located nucleus (Davis and Dickey 2008; Birchenough et al. 2015).

In the present studies, the opportunity was taken to examine the goblet cells from a cytological perspective and using Giemsa to define the cells. The IC samples for this study were taken immediately after euthanasia of the animals used, but have also be taken from living rabbits as well (reviewed in Doughty, 2015a). The cytological approach reveals the goblet cell outline and its nucleus but the mucus content is not stained. The result is a cell with essentially no staining of the cytoplasm so giving a balloon-like appearance which can also be seen in IC specimens stained with haematoxylin (Rath et al. 2006), modified Papanicolaou stain (Zuazo et al. 2014; Izci et al. 2015), and also following use of certain immunocytochemical staining procedures (Krenzer and Freddo, 1997; Danjo et al. 1998). With such well resolved visualization of the goblet cells, measures of cell dimensions and areas can be easily undertaken, especially if the extra step of substantially magnifying the final images (by projection) is also undertaken. This is hopefully evident in Figure 1, where the process of drawing the outline of the goblet cell onto an overlay is shown. An obvious number of goblet cells in a 200 X microscope field of view was only evident if, as shown in Figure 1 (and Figure 2B), two or three layers of conjunctival cells had adhered to the filter (Doughty, 2015a). If only the most superficial cells attached to a particular region of the filter surface, then some of the gaps between the cells (as shown in Figure 2A) might be considered to be where some superficially-located goblet cells might have been located. However, as considered in detail elsewhere (Doughty, 2015a), the gaps between some cells more likely indicate simply that superficial non-goblet cells did not adhere to the filter initially or stay fixed during processing. It has been proposed that such apparent separation between non-goblet cells should not only be assessed as part of assigning a subjective grade to the specimens but this ‘quality of cell-to-cell adhesion’ could be an (early) indicator the squamous metaplasia of the non-goblet cells (Haller-Schober et al., 2006). However, a case has also been made that if the slightly separated cells do not show signs of enlargement and notable change in the nucleo-cytoplasmic ratio, both of which are logically the dominant features of squamous metaplasia) (Doughty, 2015b), then this feature of the IC sample (i.e. the apparent cell separation) is essentially an artefact of the cell collection method. That this is the case for the cells shown in Figure 2A is underpinned by the morphometry of these non-goblet epithelial cells which have sizes consistent with normal superficial cells of the bulbar conjunctiva.

The measures and analyses undertaken in the present study indicate that in normal healthy conjunctiva the nucleus of goblet cells is predictably smaller than that in surrounding epithelial (non-goblet) cells, and that this apparent size of the goblet cell nuclei is predictably dependent on the overall size of the goblet cells. This inter-dependency of apparent nucleus size to overall size could be linked to the progressive maturation of goblet cells as they migrate through their epithelia to their respective surface. A partial aspect of this could also include any changes in goblet cells that occur just before discharge of mucus content. As assessed in some detail elsewhere (Halm and Halm 2000; Liu et al. 2015), any such maturation-related changes in goblet cells can include expansion of the mucin content. In the present study, it is assumed that differences in the overall size of the goblet cells can also indicate differences in their mucin content. From this perspective, the overall nature of the size-related change in the nucleo-cytoplasmic area fraction could indicate a proportional increase in mucin area (content), in part as a result of a compensatory reduction in nucleus area. It has been stated that animal goblet cells can have ‘big’ nuclei although no morphometry data was reported (Raji and Naserpour 2007), while goblet cell nucleus diameter has actually been measured in human tissue sections assessed by transmission electron microscopy (Mercer et al. 1994) with average values of 9.3 μm being reported. From serial sections examined by transmission electron microscopy, the

goblet cell volume in rabbit bulbar conjunctiva has been estimated to be 1160 μm^3, while the nucleus had a volume of just 73 μm^3 (Hirosawa et al. 1991), i.e. only around 5 % of total cell volume. The present studies indicate that this relative volume might be slightly higher at around 9.5 %.

Without any other substantial data on the morphometry of Giemsa-stained goblet cells, it is only possible to generally discuss the results in the context of related studies. So, for example, using periodate-Schiff (PAS) staining, which may or may not produce a well-demarcated goblet cell outline in impression cytology specimens (Doughty 2012b), the mean cell 'diameter' (for goblet cells) has been reported to be 16.4 μm (Aragona et al. 1996) or between 16.4 and 17.6 μm (Rivas et al. 1991). These values, from human rather than rabbit conjunctival samples, are similar to the mean cell diameter of 15.5 μm obtained in the present studies. In another human study, the maximum and minimum diameters for goblet cells were reported to be 18.9 and 14.6 μm respectively, with an average area of 193 μm^2 (Moreno et al. 2003); these values are also broadly consistent with the results from the present study. However, in another human study, the area of the goblet cells (based on PAS staining) was reported to be 408 μm^2 (Rivas et al. 2002), i.e. twice the size seen in the present studies on rabbit conjunctiva. Using transmission electron microscopy to examine serial sections through rabbit conjunctiva, an estimate of goblet cell volume was given as 1160 μm^3, albeit from just 5 different ells (Hirosawa et al. 1991); this value is rather smaller that the estimated volume of 1885 μm^3 (from 150 different goblet cells) in the present studies. Volume estimates for the whole goblet cells of around 2500 μm^3 have been reported from human tissue sections, without serial sectioning, evaluated by transmission electron microscopy (Mercer et al. 1994).

Overall, in assessments of the impression cytology filters to be used for measures of goblet cell size and shape, just those regions where there was not very substantial multilayering of the cells were selected. This allows for good resolution imaging of the goblet cells and their nuclei, an attribute not always possible when several cell layers (i.e. 4 or probably more) [Doughty, 2015a] were removed onto the filter. In the latter regions, while the outline of the goblet cells was still usually very distinctive, obtaining an in-focus image of the nucleus was much more difficult and perhaps only 2 or 3 goblet cells in any particular field of view would be suitable for morphometry of the nuclei. Overall, as illustrated previously (Doughty 2015a), the apparent size of the goblet cell appears to be dependent on the actual number (density) of goblet cells visible in a field of view, i.e. the higher the number of goblet cells, the smaller their size. Further studies are needed to assess this variable whether this be based on a cytological perspective or using conventional histological methods. The smaller goblet cells might be those located deeper in the epithelial cell layer (Doughty 2012b, 2015a).

In conclusion, the present studies indicate that the apparent size (and volume) of the goblet cell nuclei is predictably dependent on the overall size (and estimated volume) of conjunctival goblet cells. These studies need to be extended to normal human (or other animal) conjunctival specimens, and could provide both an indicator of goblet cell maturity, as well as basis for assessments of whether this feature of the goblet cells is altered in conditions such as dry eye. These conclusions are only directly applicable to conjunctival goblet cells, and it would be useful for some comparative data to be generated for goblet cells at other locations in the body but likely using slightly different cytological or histological techniques.

References

Aragona P, Romeo GF, Puzzolo D, Micali A, Ferreri G. (1996) Impression cytology of the conjunctival epithelium in patients with vernal conjunctivitis. *Eye* 10; 82-85.

Birchenough GMH, Johansson MEV, Gustafsson JK, Bergstom JH, Hansson GC (2015) New developments in goblet cell mucus secretion and function. *Mucosal Immunology* 8: 712-719.

Boucherat O, Boczkowski J, Jeannotte L, Delacourt C (2013) Cellular and molecular mechanisms of goblet cell metaplasia in the respiratory airways. *Exptl. Lung Res*. 39: 207-216.

Carillo MP, Martinez NH, Del Pilar Patiño M, Iregui CA (2015) Inhibition of Pasteurella multicoda adhesion to rabbit respiratory epithelium using lectins. **Vet. Med. Int**. 2105; Article ID 365428.

Colorado LH, Alzahrani Y, Pritchard N, Efron N (2016) Assessment of conjunctival goblet cell density using laser scanning confocal microscopy versus impression cytology. *Contact Lens Anterior Eye* – in pres; doi.org/10.106/j.clae.2016.01.006

Danjo Y, Watanabe H, Tisdale AS, George M, Tsumura T, Abelson MB, Gipson IK (1998) Alternation of mucin in human conjunctival epithelia in dry eye. *Invest. Ophthalmol. Vis. Sci.* 39: 2602-2609.

Davis CW, Dickey BF (2008) Regulated airway goblet cell mucin secretion. Ann Rev Physiol. 70: 487-512.

Doughty MJ (2011) Contact lens wear and the goblet cells of the human conjunctiva – a review. *Contact Lens Anterior Eye* 34: 157-163.

Doughty MJ (2012a) Sampling area selection for the assessment of goblet cell density from conjunctival impression cytology specimens. *Eye Contact Lens* 38: 122-129.

Doughty MJ (2012b) Goblet cells of the normal human bulbar conjunctiva and their assessment by impression cytology. *Ocular Surface* 10: 149-169.

Doughty MJ (2014) Functional morphology of mucosal goblet cells based on spatial separation of orifice openings to the surface – application to rabbit bulbar conjunctiva. *Tissue Cell* 46: 241-248.

Doughty MJ (2015a) A systematic assessment of goblet cell sampling of the bulbar conjunctiva by impression cytology. *Exp. Eye Res*. 136: 16-28.

Doughty MJ (2015b) Assessment of consistency in assignment of severe (grade 3) squamous metaplasia to human bulbar conjunctival impression cytology cell samples. Ocular Surface 13|: 284-297.

Forstner G (1995) Signal transduction, packaging and secretion of mucins. *Annu. Rev. Physiol.* 57: 585-605.

Haller-Schober E-M, Schwantzer G, Berghold A, Fischl M, Theisel A, Horwath-Winter J (2006) Evaluating an impression cytology grading system (IC Score) in patients with dry eye syndrome. *Eye* 20: 927-933.

Halm DR, Halm ST (2000) Secretagogue response of goblet cells and columnar cell in human colonic crypts. *Am. J. Physiol. Cell Physiol.* 278: C212-C233.

Hirosawa K, Kasamatsu Y, Shiraishi T (1991) Three-dimensional reconstruction of goblet cells in the rabbit conjunctivum. *J. Electron Microsc*. 40: 54-57.

Izci C, Celik I, Alkan F, Erol M, Sur E (2105) Clinical and light microscopic studies of the conjunctival tissues of dogs with bilateral keratoconjunctivitis sicca before and after treatment with topical 2 % cyclosporine. *Biotechnic Histochem.* 90: 223-230.

Johansson MEV (2012) Fast renewal of the distal colonic mucos layers by the surface goblet cells as measured by in vivo labeling of mucin glycoproteins. *PLoS ONE* 7: e41009.

Kandori H, Hirayama K, Takeda M, Doi K (1996) Histochemical, lectin-histochemical and morphometrical characteristics of intestinal goblet cells of germfree and conventional mice. *Exp. Anim.* 45: 155-160.

Karam SM (1999) Lineage commitment and maturation of epithelial cells in the gut. *Frontiers Biosci.* 4: d286-d298.

Kim YS, Ho SB (2010) Intestinal goblet cells and mucins in health and disease: Recent insights and progress. *Curr. Gastroenterol. Rep*. 12: 319-330.

Krenzer KL, Freddo TF (1997) Cytokeratin expression in normal human bulbar conjunctiva obtained by impression cytology. *Invest. Ophthalmol. Vis. Sci.* 38:142-152.

Kumari U, Yashpal M, Mittal S, Mittal AK (2009) Histochemical analysis of glycoprotiens in the secretory cells in the gill epithelium of a catfish, Rita rita (Siluriformes, Bagridae). *Tissue Cell* 41: 271-280.

Lin RY, Nahal A, Lee M, Clarin E, Menikoff H (1998) Clinical predictors of nasal secretory cell quantities in allergy clinic patients. *Ann. Allergy Asthma Immunol.* 80: 477-482.

Liu J, Walker NM, Ootani A, Strubberg AM, Clarke LL (2015) Defective goblet cell exocytosis contributed to murine cystic fibrosis-associated intestinal disease. *J. Clin. Invest.* 125: 1056-1058.

Martins C, Alves de Matos A, Costa MH, Costa PM (2015) Alterations in juvenile flatfish epithelia induced by sediment-bound toxicants: A comparative in situ and ex situ study. *Marine Environm. Res.* 112: 122-130.

Mercer RR, Russell ML, Roggli VL, Crapo JD (1994) Cell number and distribution in human and rat airways. *Am. J. Respir. Cell Mol. Biol.* 10: 613-624.

Moreno M, Villena A, Cabarga C, Sanchez-Font E, Garcia-Campos J (2003) Impression cytology of the conjunctival epithelium after antiglaucomatous treatment with latanoprost. *Eur. J. Ophthalmol*. 13: 553-559.

Pagliuca G, Rosato C, Martellucci S, De Vincentiis M, Greco A, Fusconi M, De Virgilio A, Gallipoli C, Simonelli M, Gallo A (2016) Cytologic and functional alterations of nasal mucosa in smokers: Temporary or permanent damage ?. *Otolaryngol. Head Neck Surg.* 152: 740-745.

Raji AR, Naserpor M (2007) Light and electron microscopic studies of the trachea in the one-humped camel (Camelus dromedaries). *Anat. Histol. Embryol.* 36: 10-13.

R**ath R, Stave J, Guthoff R, Giebel J, Tost F** (2006) In-vivo-Darstellung des Bindehautepithels. *Ophthalmologe* 103: 401-405.

Rivas L, Oroza MA, Perez-Esteban A, Murube-del-Castillo J (1991) Topographical distribution of ocular surface cells by the use of impression cytology. *Acta Ophthalmol.* 69, 371-376.

Rivas L, Murube J, Shalaby O, Oroza MA, Sanz AI (2002) Contribución de la citología de impression al diagnóstico diferencial del síndrome de Sjögren en la clínica oftalmológica. *Arch. Soc. Esp. Oftalmol.* 77: 63-72.

Rose MC, Voynow JA (2006) Respiratory tract mucin genes and mucin glycoproteins in health and disease. *Physiol. Rev.* 86: 245-278.

Roth A, Tabatabay C, Englert U (1988) Sécrétion meibomienne et sydrome pseudo-sec. Apport de l'empreinte conjunctivale. *Ophtalmologie* 2(2):131-133.

Schroeder BW, Verhaeghe C, Park S-W, Nguyenvu LT, Huang X, Zhen G, Erle DJ (2012) AGR2 is induced in asthma and promotes allergen-induced mucin overproduction. *Am. J. Respir. Cell Mol. Biol.* 47: 178-185.

Spurzem JR, Thompson AB, Daughton DM, Mueller M, Linder J, Rennard SI (1991) Chronic inflammation is associated with an increased proportion of goblet cells recovered by bronchial lavage. *Chest* 100: 389-393.

Stringer AM, Gibson RJ, Logan RM, Bowen JM, Yeoh SJ, Hamilton J, Keefe DMK (2009) Gastrointenstinal microflora and mucins may play a critical role in the development of 5-fluorouracil-induced gastrointestinal mucositis. *Exp. Biol. Med.* 234: 430-441.

Zuazo F, López-Ponse D, Salinas-Toro D, Valenzuela F, Sans-Puroja J, Srur M, López-Solis RO, Traipe-Castro L (2014) Conjunctival impression cytology in patients with normal and impaired OSDI scores. *Arch. Soc. Esp. Oftalmol.* 89: 391-396.

Figure captions

Figure 1. Photograph to illustrate conjunctival cytology image projection from which overlays were prepared for morphometry. The image shows a field of view at approximately 1000 X final magnification including flat epithelial (non-goblet) cells and the distinctive balloon-like (spheroid-like) goblet cells highlighted with Giemsa stain.

Figure 2. Portions of images of epithelial (non-goblet) cells with large nucleus (arrow) (A) and mixture of epithelial cells and the balloon-like goblet cells with smaller eccentrically-located nuclei (arrow) (B). The height of the vertical box (scale bar) is 100 μm.

Figure 3. Histograms to show distribution of the longest dimension of goblet cells (A) and the shape of the goblet cells, based on the ratio of the longest dimension to shortest dimension L:S ratio (B).

Figure 4. Goblet cell area and its predictability. (A) histogram of measured goblet cell areas, (B) scatterplot to show comparison between measured goblet cell areas and estimated goblet cell areas calculated from the 'average' diameter, (C) utility of the longest dimension of the goblet cells to predict goblet cell area (using calculations based on 'average' diameter).

Figure 5. Goblet cell nucleus area values (A) and the dependence of the nucleo-cytoplasmic area fraction (calculated from goblet cell nucleus area / cell cytoplasm area) on the total goblet cell area.

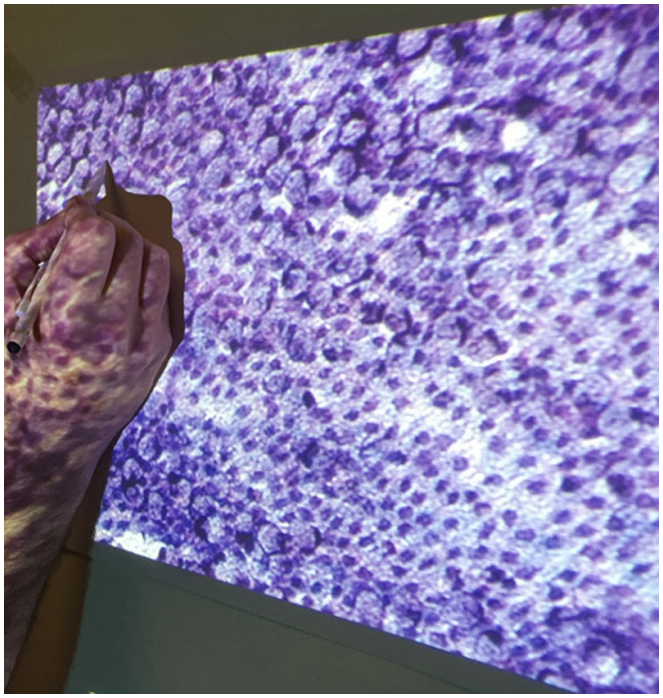

FIGURE 1

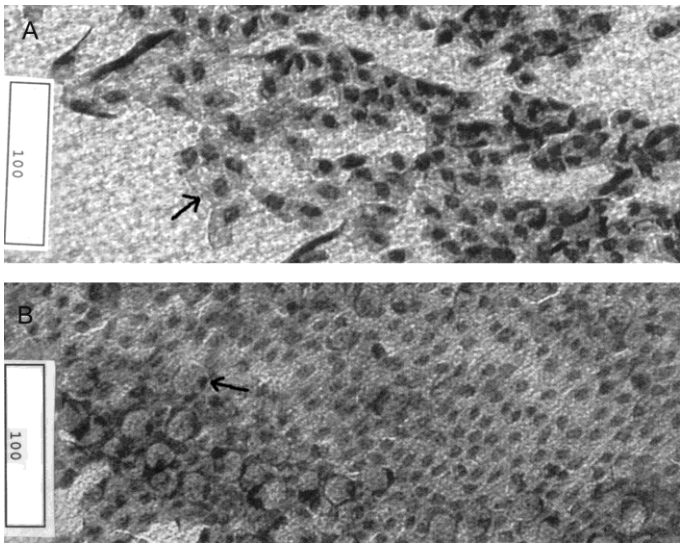

FIGURE 2

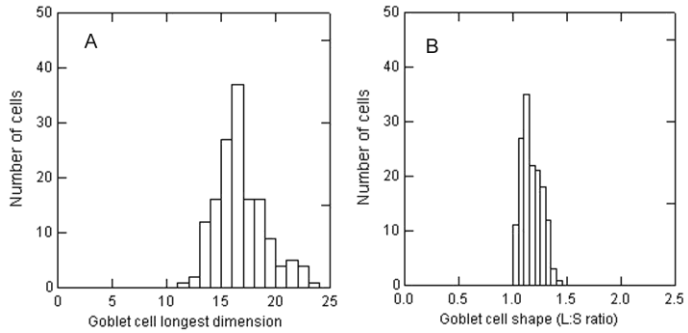

FIGURE 3

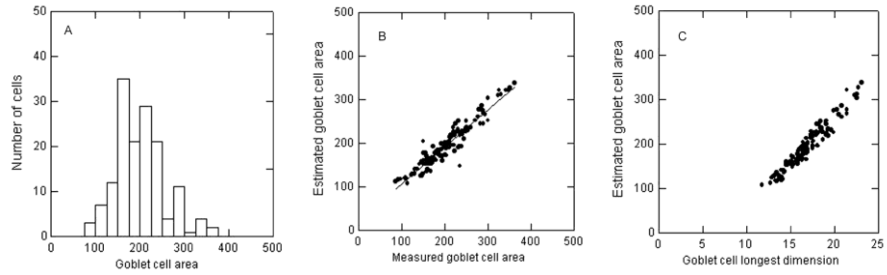

FIGURE 4

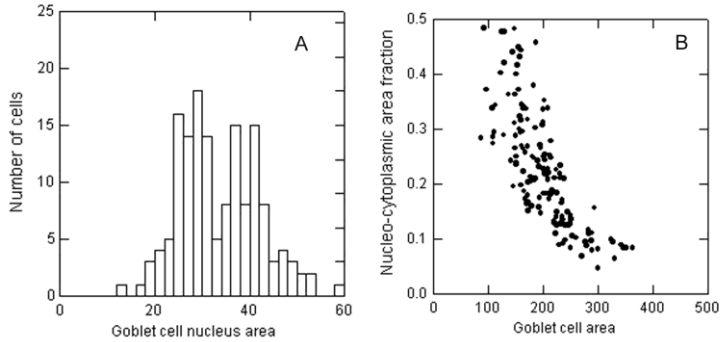

FIGURE 5